Bayes Information Criterion for Tikhonov Problems with Linear Constraints: Application to Radiometric Image Correction

P. Carvalho, A. Santos, A. Dourado, B. Ribeiro
Centre for Informatics and Systems, University of Coimbra
Pólo II, Pinhal de Marrocos, 3030 Coimbra, Portugal
Email: {carvalho, amancio, dourado, bribeiro}@dei.uc.pt

ABSTRACT
Ill-conditioned or singular data modeling problems are commonly observed in image processing. To solve these problems some constraints, such as smoothness and boundary conditions have to be formulated. Further, the optimal structure of the model is not always self-evident. There are several criteria that can be applied for "optimal" regularization gain or model selection. However, these measures (i) are not for problems with linear constraints and, further (ii) are usually not simultaneously suitable for model and regularization gain selection. In this paper the Bayes Information Criterion is extended for Tikhonov problems with linear constraints. Using this measure, a new radiometric image correction method is introduced. All known radiometric correction algorithms assume that radiometric distortions remain stable over time. Our algorithm enables image correction under time varying distortions. The method decomposes radiometric image distortions into multiplicative and additive errors, whose optimal models are computed with the extended Bayes Information Criterion (BIC_{IC}).

KEY WORDS
Machine Learning, Image Correction, Camera Calibration.

1 Introduction

Ill-posed or singular linear problems are commonly observed in many image processing and computer vision situations, where (i) few linear independent data exist for the estimation problem and (ii) the observed data are the result of an integration process such as convolution. This type of problems arise in several contexts, such as in camera calibration [1], reflectance estimation [1], and image restoration [2], just to name a few. To solve these problems some additional information is necessary. In most cases, the solution is required to exhibit some set of characteristics, being the most common the smoothness of some function, curve or surface build upon it. If smoothness is encoded with a quadratic penalty involving derivatives such as $\gamma \int \left(f^{(w)}(x) \right)^2 dx$ ($f^{(w)}(x)$ is the model's wth order derivative and γ is the regularization gain), then the method is commonly referred to as Tikhonov regularization. Other type of constraints are due to physical properties, such as boundary conditions, shape, etc., usually described with

linear inequalities. In some other data modeling problems enough linear independent data exist, but the underlying physical process is not well understood. In these cases several models must be fit to the data and the best model has to be selected from these competing models. This problem arises in many computer vision situations, such as in lens calibration [3], selection of deformation models to describe deviations from CAD specifications in inspection tasks and surface reconstruction for 3D modelling (see [4] and references therein). If proper model and regularization gain are known *a priori*, then such data modeling problems are readably solvable. However, in most practical situations, this knowledge is unavailable. Hence, some criterion is required to select those parameters. There are several criteria based on the bias-variance/complexity trade-off principle (BIC [5], AIC [6], GCV [6], etc.), for regularization gain or model selection. However, these measures (i) are not for problems with linear constraints and, further (ii) are usually not suitable for both selection operations. In section 2 the Bayes Information Criteria, originally introduced by Schwartz [5] and later extended by Neath and Cavanaugh [7] for model selection in well-defined regression problems, is extended in this context and applied to radiometric image correction.

Radiometric image distortions are due to multiplicative errors, induced by variations in amplification gain and by the sensor's photo response nonuniformities (PRNU), and due to additive errors, which are mainly caused by blackcurrent, by internal luminance and fat zero. The later are very prone to temperature variations. For instance, for solid-state sensors it is usually observed that blackcurrent approximately doubles for every 8^oC. On the other hand, gain variations have been reported, even when automatic gain is turned off [8]. Hence, in real world applications these time varying distortions should be corrected. Areas where this premise is important are color vision [1], 3D vision [9] and image restoration applications [2], just to name a few. There are several approaches to radiometric image correction. Healey and Kondepudy [10] have identified the main noise sources, which occur in the image formation process, and have described an algorithm for radiometric distortion assuming static noise characteristics. In practice, as will be shown, this behavior is only verified under very restricted conditions. Other methods have been proposed

for radiometric image correction, which rely on the same premises. Kamberova and Bajcsy [9] identify linear image transformations such that for an uniform surface, all pixels in the corrected image exhibit equal values.

In section 3, a new method for radiometric image distortion correction, that does not rely on the static behavior of noise characteristics, is presented. The proposed method operates in two stages (see figure 1). (i) During a calibration phase, distortion models for multiplicative and additive errors are identified. (ii) These models are then applied to correct each acquired image. Time varying multiplicative image distortions are captured from a controlled image region. Since these gain variations are global to the image, its correction is straightforward. To capture variations in additive errors a different approach has to be applied, since these changes are a property of each pixel. Additive error can readably be computed for controlled image regions, i.e., regions where the sensor's cells light stimulus is kept constant over time. From these controlled sensor cells, variation in additive error can be identified and used as input to the calibrated error models which relate these variations to those observed in each cell of the sensor. For most visual inspection applications, this can be achieved with reference surfaces, since usually in these situations controlled artificial light is applied. For general computer vision situations, constant light stimulus can be achieved by avoiding light exposure of these sensor cells, for instance using a neutral density filter or by covering that section of the sensor. If this approach is applied, gain compensation is no longer feasible. However, good correction results can still be obtained with this strategy, if automatic gain is turned off.

2 Model and regularization gain selection with BIC_{IC}

Let us assume the general formulation of a Tikhonov regularization problem using a regularized empirical risk functional subject to linear inequality constraints, as in (1) and in (2).

$$\min_x \left\{ \frac{1}{2m} \|Ax - y\|^2 + \frac{\gamma}{2} \|Dx\|^2 \right\}, \gamma \in \mathbb{R}^+ \quad (1)$$

$$\Xi \equiv \{C_i x \le d_i : i = 1, ..., k\} \quad (2)$$

Suppose n defines the order of the linear model to be identified from the known data $Y \equiv \{(z_i, y_i), i = 1, ..., m\}$, and γ controls the trade-off between the data fidelity $\|Ax - y\|^2$ and the smoothness $\|Dx\|^2$ of the model. Further, let us assume $A \in \mathbb{R}^{m \times n}$, $x \in \mathbb{R}^n$, $y \in \mathbb{R}^m$, $D \in \mathbb{R}^{l \times n}$, $l \ge n$, $n \ge rank(D)$, where Dx is a discrete approximation to $f^{(w)}(x)$, and $C \in \mathbb{R}^{k \times n}$. Given a set of parameters (γ, n) and constraints Ξ, the optimal solution can be obtained using active set algorithms (see [11]). However, in most situations, this *a priori* knowledge is unavailable. In practice it is seen that if n is too small, then
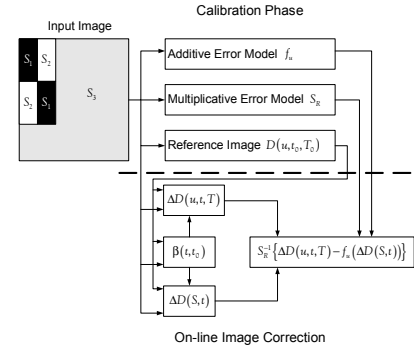
Figure 1. Overview of the radiometric correction method.

underfitting may occur, while if n is too large, then usually overfitting is observed. On the other hand, if $\gamma \to 0$ then, for ill-posed problems the estimated model tends to exhibit high frequency oscillation and, therefore, it cannot be applied for interpolation. If $\gamma \to \infty$, then a line is identified, if Dx is a discrete approximation to $f^{(2)}(x)$. Hence, estimating the optimal values for γ, n and Ξ is critical.

In this section the Bayes Information Criteria is extended for the selection of γ, n and Ξ in problem of (1) and (2). A similar strategy as applied in [7] for the ordinary BIC is followed. Since the quadratic penalty in (1) can be seen as a quadratic constraint, for notation simplicity, all constraints are defined by $\Sigma \equiv (\Xi, \gamma)$. Let $P(Y|x, n, \Sigma)$ the likelihood for Y based on x, n and Σ. Furthermore, let $P(n|\Sigma)$, $P(\Sigma)$, $P(x|n, \Sigma)$ be prior distributions, respectively, for the model of dimension n, given Σ, for the constraints, and for the model's parameterization vector, given n and Σ. The joint a posteriori distribution for x, n and Σ given the observed data Y can be obtained with the Bayes rule by (3), where the marginal distribution $h(Y) \equiv \sum_n \int \int P(Y, x, n, \Sigma) dx d\Sigma$.

$$f(x, n, \Sigma|Y) = \frac{P(n|\Sigma) P(\Sigma) P(Y|x, n, \Sigma) P(x|n, \Sigma)}{h(Y)} \quad (3)$$

Using this result, to select proper model order n and constraints Σ, one expects the a posteriori distribution $f(n, \Sigma|Y)$ to be maximized, or equivalently

$$\min_{n, \Sigma} \left\{ -2 \ln \left(\int f(x, n, \Sigma|Y) dx \right) \right\} \quad (4)$$

In order to solve the integral in equation (4), $P(Y|x, n, \Sigma) P(x|n, \Sigma)$ has to be determined. Let $\widehat{C}x = \widehat{d}$, $\widehat{C} \in \mathbb{R}^{p \times n}$, $rank\left(\widehat{C}\right) = p < n$ (note that if $p = n$ the solution is uniquely obtained from the constraints), be the active set of constraints, i.e. constraints verified with equality, at the solution of (1) and (2) computed for a particular set of parameters (Σ, n). If these constraints are known, then the solution is easily computed from the following theorem.

Theorem 1: Let $B \in \mathbb{R}^{t \times n}$, $t \geq n$, $G \in \mathbb{R}^{p \times n}$, $p = rank\{G\}$, and $rank\left\{\left(B^T, G^T\right)^T\right\} = n$. The best approximate solution to the equality constrained problem in (5) is (6),

$$\min_x \left\{\|Bx - e\|^2\right\} \text{ subject to } Gx = h \qquad (5)$$

$$x = Z^{-1}\left(w_1^T, w_2^T\right)^T \qquad (6)$$

where $w_1 = D_G^{-1} V^T h \in \mathbb{R}^p$, $w_2 = \left(0, D_{B_2}^{-1}, 0\right) U^T e \in \mathbb{R}^{n-p}$, and $B = U\left(D_B^T, 0\right)^T Z$ and $G = V\left(D_G, 0\right) Z$ are the generalized singular value decompositions of matrixes B and G,

$$D_B = \begin{pmatrix} D_{B_1} & 0 \\ 0 & D_{B_2} \end{pmatrix}$$

$D_{B_1} = diag\left(\alpha_1, ..., \alpha_p\right)$, $D_{B_2} = diag\left(\alpha_{p+1}, ..., \alpha_n\right)$, $D_G = diag\left(\beta_1, ..., \beta_p\right)$, $U \in \mathbb{R}^{t \times t}$ and $V \in \mathbb{R}^{p \times p}$ are unitary orthogonal matrixes, and $Z \in \mathbb{R}^{n \times n}$ is a matrix of $rank$ n. Further, it is observed that w_2 can be computed from

$$\min_{w_2}\left\{\|Hw_2 - \widetilde{e}\|^2\right\} \qquad (7)$$

where $H = U\left(0, D_{B_2}^T, 0\right)^T \in \mathbb{R}^{t \times (n-p)}$ and $\widetilde{e} \equiv e - U\left(\left(D_{B_1} D_G^{-1} V^T h\right)^T, 0\right)^T$. (Partial proof of equation (6) is given in [11]. As for equation (7), it is obtained by substituting w_1 in (5) and performing some simple algebraic manipulations.)

Using theorem 1, it follows that (1) is equivalent to $\min_{w_2} \frac{1}{2m}\|Hw_2 - \widetilde{e}\|^2$, with $B^T \equiv \left(A^T, \sqrt{\gamma m} D^T\right)$, $e^T \equiv \left(y^T, 0\right)$, $G \equiv \widehat{C}$, $h \equiv \widehat{d}$. Substituting this result into (4) and eliminating constant terms hilts

$$BIC_{IC}(n, \Sigma) = -2\ln P(n|\Sigma) - 2\ln P(\Sigma) \qquad (8)$$
$$-2\ln \int P(Y|w_2, n, \Sigma) P(w_2|n, \Sigma) dw_2$$

To compute the integral in (8), a second order Taylor approximation of $P(Y|w_2, n, \Sigma) P(w_2|n, \Sigma)$ can be used. Let $\widehat{w}_2$ be the maximum likelihood estimate vector of $\widehat{w}_2$ obtained from $\max_{w_2}\{P(Y|w_2, n, \Sigma) P(w_2|n, \Sigma)\}$, then $\ln P(Y|w_2, n, \Sigma) P(w_2|n, \Sigma)$ can be approximated for a region near $\widehat{w}_2$ as in (9), where $F(w_2)$ is the Hessian matrix defined in (10).

$$\ln P(Y|w_2, n, \Sigma) P(w_2|n, \Sigma) \approx$$
$$\ln P(Y|\widehat{w}_2, n, \Sigma) P(\widehat{w}_2|n, \Sigma) - \frac{(w_2 - \widehat{w}_2)^T F(\widehat{w}_2)(w_2 - \widehat{w}_2)}{2}$$
$$(9)$$

$$F(w_2) \equiv -\frac{\partial^2 \ln P(Y|w_2, n, \Sigma) P(w_2|n, \Sigma)}{\partial w_2 \partial w_2^T} \qquad (10)$$

From (9) it follows that

$$P(Y|w_2, n, \Sigma) P(w_2|n, \Sigma) \approx$$
$$P(Y|\widehat{w}_2, n, \Sigma) P(\widehat{w}_2|n, \Sigma) \exp\left(-\frac{(w_2 - \widehat{w}_2)^T F(\widehat{w}_2)(w_2 - \widehat{w}_2)}{2}\right)$$
$$(11)$$

Hence, it is observed that

$$\int P(Y|w_2, n, \Sigma) P(w_2|n, \Sigma) dw_2 \qquad (12)$$
$$\approx P(Y|\widehat{w}_2, n, \Sigma) P(\widehat{w}_2|n, \Sigma) (2\pi)^{\frac{n-p}{2}} |F(\widehat{w}_2)|^{-\frac{1}{2}}$$

Combining (12) with (8), the BIC_{IC} criterion can be described by

$$BIC_{IC}(n, \Sigma) = -2\ln P(n|\Sigma) - 2\ln P(\Sigma) \qquad (13)$$
$$-2\ln P(Y|\widehat{w}_2, n, \Sigma) P(\widehat{w}_2|n, \Sigma)$$
$$-(n-p)\ln 2\pi + \ln|F(\widehat{w}_2)|$$

Note that due the non parametric nature of the problem (7) implies (14) (see [12]), which leads to $F(\widehat{w}_2) = m^{-1} H^T H$.

$$P(Y|w_2, n, \Sigma) P(w_2|n, \Sigma)$$
$$\propto \exp\left\{-\frac{1}{2m}\left(\|Hw_2 - \widetilde{e}\|^2\right)\right\} \qquad (14)$$

Hence, plugging (14) and $F(\widehat{w}_2)$ into (13), (15) follows.

$$BIC_{IC}(n, \Sigma) = -2\ln P(n|\Sigma) - 2\ln P(\Sigma)$$
$$-(n-p)\ln 2\pi m + \frac{1}{m}\|H\widehat{w}_2 - \widetilde{e}\|^2 + \ln\left|H^T H\right|$$
$$(15)$$

3 Radiometric distortion correction

Let $D(u, t, T)$ be the linearized camera output for point of coordinates $u \in \mathbb{N}^2$ at instant t and temperature T, then

$$D(u, t, T) = \overline{D}(u, t, T) + N(u, t, T) \qquad (16)$$

where $N(u, t, T)$ is a random variable of mean zero and variance $\sigma_N^2(u, t, T)$ induced by shot, read and quantization noise and

$$\overline{D}(u, t, T) = A(t) S_R(u) I(u, t) + A(t) O(u, T) + N_F(u) \qquad (17)$$
$$O(u, T) \equiv N_D(u, T) + N_{FZ}(u) + N_{IL}(u, T)$$

In (17) $A(t)$, $S_R(u)$, $N_D(u, T)$, $N_{FZ}(u)$, $N_{IL}(u, T)$ and $N_F(u)$ represent, respectively, the channel's gain, the fixed pattern noise or photo response non uniformities (PRNU) in charge collection, the dark current charge, fat zero, internal luminance and the offset introduced by the camera's transfer function and the digitizer for pixel u. $I(u, t)$ is defined as $\int_{\lambda_0}^{\lambda_n} I(\lambda, u, t) S(\lambda) d\lambda$, where $I(\lambda, u, t)$ is the SPD (spectral power distribution) of the input radiation at point u and instant t and $S(\lambda)$ is the spectral sensitivity of the image sensor. For cameras with almost linear transfer functions (most common in scientific and industrial applications), it can be shown that $N_F(u)$ is approximately constant, since it mainly describes the offset introduced by the digitizer.

In figure 2 several line statistics of dark images (images taken with the lens cap on) obtained under different
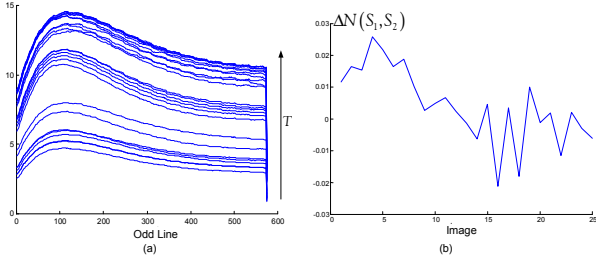
Figure 2. Intensity variation of dark images obtained with a Sofretec CF 820 camera for distinct environment temperatures $T \in [6, 20]^\circ C$. (a) Average intensity for odd lines. (b) Variation of ΔN for a sequence of 25 images taken with $T \in [6, 20]^\circ C$.

environment temperatures with a Sofretec CF 820 CCD camera are shown. As can be observed, an environment temperature change of $14^\circ C$ induces a variation in $O(u, T)$ over 300% for this camera.

To perform radiometric image correction, for each image the multiplicative errors $S_R(u)$ and $A(t)$, and the additive error $A(t)O(u, T) + N_F(u)$ have to be estimated. Let $A(t_0)$ be the channel's gain for a reference image $D(u, t_0, T_0)$. Instead of computing the absolute values for the camera's gain and offset error, in this correction approach, relative values $\beta(t, t_0) = A(t)/A(t_0)$ and $\Delta D(u, t) = A(t_0) \{O(u, T) - O(u, T_0)\}$ are identified.

Let us assume that each image is composed by three different regions S_i, $i = 1, .., 3$, such that S_1 and S_2 form a chess pattern as shown in figure 1. Further, let us assume that for the first two regions S_1 and S_2, no changes in $I(\lambda, u, t)$ occur, i. e., the illumination $I_E(\lambda)$ and the reflectance characteristics $R(\lambda, u, t)$, $(u, v) \in \{S_1, S_2\}$, of the imaged surfaces are kept constant over time. The image data in regions S_1 and S_2 enable the estimation of $\Delta D(u, t)$ and $\beta(t, t_0)$. Let $D(S_i, t, T) \equiv (s(t) \|S_i\|)^{-1} \sum_{u \in S_i} \sum_{t_w \in s(t)} D(u, t_w, T_w)$ be the average image intensity in region S_i, where $s(t)$ and $\|S_i\|$ are respectively the number of images taken and the number of pixels in region S_i. Evaluating the difference between mean intensities in regions S_1 and S_2, it is seen that ($C_{LI}(u) I_i \equiv I(u, t)$, $u \in S_i$, $i = 1, 2$, $C_{LI}(u) \in [0, 1]$ accounts for geometric power distribution of (i) the light source, (ii) the reflection and (iii) the lens attenuation),

$$Z(S_1, S_2, t, T) \equiv D(S_2, t, T) - D(S_1, t, T) = \frac{A(t)}{s(t)\|S_i\|} \left\{ I_2 \sum_{u \in S2} C_{LI}(u) S_R(u) \right. \quad (18)$$
$$\left. - I_1 \sum_{u \in S1} C_{LI}(u) S_R(u) \right\} + \Delta N(S_2, S_1)$$

In practice, given that both regions S_1 and S_2 share the same columns and lines of the image (due to the chess pattern), it is observed that $\Delta N(S_2, S_1) \to 0$, as can be seen in figure 2 (c). Hence, as long as $I_1 \ll I_2$, it follows that (18) enables the estimation of the relative gain variation

$\beta(t, t_0)$:

$$\beta(t, t_0) \equiv \frac{Z(S_1, S_2, t_0, T_0)}{Z(S_1, S_2, t, T)} \quad (19)$$

If $\|S_1\| = \|S_2\|$ and $s(t_0)$ is taken large enough such that the uncertainty in (19) is mainly conditioned by the data at instant t, it can be shown that the expected value for $\beta(t, t_0)$ and its uncertainty can be computed as in (20) and (21), where $\sigma_{S_i}^2(t) \equiv (s(t) \|S_i\|)^{-1} \sum_{u \in S_i} \sum_{t_w \in s(t)} \sigma_N^2(u, t_w, T_w)$ is the average noise variance in region S_i.

$$E[\beta(t, t_0)] \simeq A(t)^{-1} A(t_0) \quad (20)$$

$$V[\beta(t, t_0)] \simeq \frac{\left(\sigma_{S_1}^2(t) + \sigma_{S_2}^2(t)\right) E[Z(S_1, S_2, t, T)]^2}{s(t) \|S_1\| E[Z(S_1, S_2, t, T)]^4} \quad (21)$$

On the other hand, the change in the offset for region S_1 can be computed from $\Delta D(S_1, t) = \beta(t, t_0)^{-1} D(S_1, t, T) - D(S_1, t_0, T_0)$, which leads to

$$E[\Delta D(S_1, t)] \simeq A(t_0) \{O(S_1, T) - O(S_1, T_0)\} \quad (22)$$

$$V[\Delta D(S_1, t)] \simeq \sigma_{S_i}^2(t) E[\beta(t, t_0)]^2 + \quad (23)$$
$$V[\beta(t, t_0)] E[D((S_1, t, T))]^2$$

From (21) and (23) it is concluded that, in order to minimize the uncertainty of these estimates, the reference surfaces should be chosen such that their reflectance $R(\lambda, u, t) \to 0$, $u \in S_1$, and $R(\lambda, u, t) \to 1$, $u \in S_2$, i.e., a black and a white reference surface, respectively. Taking a similar approach for the image in region S_3, it follows that $\Delta D(u, t) = \beta(t, t_0)^{-1} D(u, t, T) - D(u, t_0, T_0)$. Hence,

$$E[\Delta D(u, t)] \simeq A(t_0) S_R(u) I(u, t) \quad (24)$$
$$+ A(t_0) (O(u, T) - O(u, T_0))$$

Note that (24) implies that $I(u, t_0) = 0$, $u \in S_3$, i. e., the reference image for region S_3 is taken without light exposure of the sensor. On the other hand, to be able to compute the change in gain $\beta(t, t_0)$ using (20), it is imperative that $I(u, t_0) \neq 0$, $u \in \{S_1, S_2\}$. This can be accomplished if the reference image $D(u, t_0, T_0)$ is obtained from two distinct images with the same sensor temperature. From the first image, acquired with the sensor exposed to light, the data for $D(u, t_0, T_0)$, $u \in \{S_1, S_2\}$, are taken, while from the second image, captured with the lens cap one, pixels $D(u, t_0, T_0)$ for region S_3 are estimated. To avoid distinct gains $A(t)$ for the two images, these should be computed from an average of a large sequence of images acquired with automatic gain disabled. Equations (22) and (24) are the basis of the correction method. Namely, if the mappings $w = f_u(\Delta D(S_1, t))$, $w \equiv A(t_0)(O(u, T) - O(u, T_0))$, are known, then an image without bias can be obtained

from $\Delta D(u,t) - f_u(\Delta D(S_1,t))$, $u \in S_3$. Since the exact physical laws which describe these mappings are unknown, a generic formulation is applied to identify f_u, i.e., $f_u(\Delta D(S_1,t)) = \sum_{i=0}^{n} x_i X_i(\Delta D(S_1,t))$, $n \in \mathbb{N}$, $x_i \in \mathbb{R}$, where X_i can be any basis function. There are some a priori knowledge that can be integrated into the estimation process to reduce the model's complexity: (i) it is seen that f_u is monotonous increasing, although not linear, and (ii) f_u should be smooth (see figure 2). The monotonous behavior is mainly due to blackcurrent. This charge follows a Boltzmann distribution, hence increases with temperature. Nonlinearity, is due to blackcurrent and due to internal illuminance generated charge. Smoothness can be imposed with a penalty term in the criterion as in (1). However, for this particular problem it is observed that the number of parameters to be estimated is usually much lower than the number of available data, i. e., $n \ll m$. Hence, to avoid the computational overhead imposed by the search for proper regularization gain, smoothness is promoted by constraining the model to exhibit a monotonous behavior, i. e., $df_u(z)/dz \geq 0$. Note that if these constraints are not imposed, then for non equally spaced data clusters, large amplitude oscillation can occur for large model orders. Hence, if a set of calibration points $\{(\Delta D(u,t_i), \Delta D(S_1,t_i)) : i = 1,...,m\}$ are known for distinct temperatures, f_u can be estimated by formulating the estimation problem in terms of least squares minimization subject to linear inequality constraints as in (25). Calibration data can be obtained from black images, i.e., images taken with the lens cap on, under different temperatures. For these images $I(u,t,\lambda) = 0$ and therefore $\Delta D(u,t) = A(t_0)(O(u,T) - O(u,T_0))$. Note that $C \in \mathbb{R}^{k \times n}$ encodes $df_u(z)/dz$ at k equally spaced points between $\min\{\Delta D(S_1,t_i)\}$ and $\max\{\Delta D(S_1,t_i)\}$, and that $A \equiv [A_1^T,...,A_m^T]^T \in \mathbb{R}^{m \times n}$, $A_i \equiv [X_1(\Delta D(S_1,t_i)),...,X_n(\Delta D(S_1,t_i))]$, $i = 1,...,m$, $y \equiv [\Delta D(u,t_1),...,\Delta D(u,t_m)]^T$, while the model's parameterization vector is defined as $x \equiv [x_1,...,x_n]^T$.

$$\min_x \left\{ \|Ax - y\|^2 \right\} : Cx \geq 0 \tag{25}$$

For a given n, the best solution can be computed from (25). However, the optimal n is not known. Using the Bayes Information Criterion for inequality constrained problems introduced in section 2, this goal can be achieved with $\min_n \{BIC_{IC}(n,\Sigma)\}$. Since all the constraints are deterministic, it is observed that $P(\Sigma) = 1$ and $P(n|\Sigma) = P(n)$. Further, given that no a priori knowledge on the optimal n is available, $P(n)$ is taken to be a uniform distribution, hence $-2lnP(n) = 0$. Finally, to compensate for PRNU noise, a similar approach as used in [10] is applied and, therefore, the corrected image can be computed as described in (26).

$$
\begin{aligned}
D_C(u) &= S_R^{-1}(u)(\Delta D(u,t) - f_u(\Delta D(S_1,t))) \tag{26}\\
&= A(t_0)C_{LI}(u) \int S(\lambda) I(u,t,\lambda) d\lambda
\end{aligned}
$$
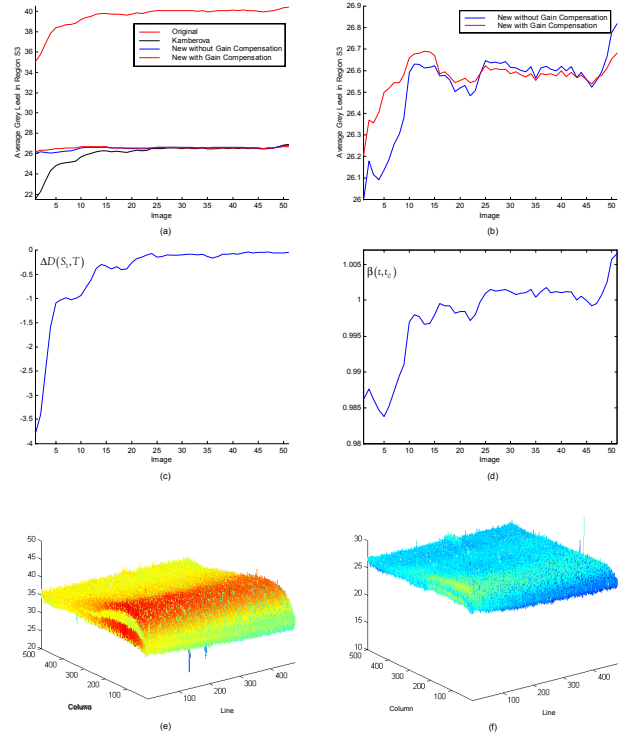
Figure 3. Patch number 22. (a) Variation of $\Delta \text{D}(S_1,t)$. (b) Variation of $\beta(t,t_0)$. (c) Comparison of correction results obtained with several methods. (d) Comparison of correction results with and without gain compensation.(e) Image number 1. (f) Correction result of image number 1 using gain compensation.

4 Results and conclusions

In figures 3 and 4 some comparisons between Kamberova's flatfielding algorithm and the described method are summarized. These results were obtained from two sequences of 51 images taken with a Sofretc CF820 CCD camera (this camera has automatic gain control), respectively, for uniformly illuminated (i) dark grey (patch number 22) and (ii) grey (patch number 21) patches of a MacBeth ColorChecker map using distinct illumination setups. For each image sequence the camera was cooled down to 0^oC during 2 hours. After this period the camera was mounted at an environment temperature of 22^oC and the image sequence was captured during the warm-up process. Each image is the result of an average of $s(t) = 100$ acquisitions. Further, the reference image was computed at $T = 22°C$, using $s(t_0) = 1000$. Therefore, the shown variance in pixel intensity after radiometric correction is mainly due to the correction process itself. The results depict in figure 3 (a)-(b) and in figure 4 are the average grey level in region S_3.

For the dark grey patch image sequence (see figure 3), it is seen that the uncorrected image sequence exhibits an average grey value variation of 5.3688 and a pixel intensity standard deviation between 2.2530 and 2.4367. As

temperature changes, static correction strategies are unable to compensate for changing noise characteristics. Namely, using Kamberova's flatfielding techniques, it is observed that the average grey value variation is similar (5.3498) to the one observed for the uncorrected image sequence, although the pixel intensity standard deviation is drastically reduced in this case (between 0.5348 and 0.9661). This is both due to PRNU correction, and the image's non uniform offset attenuation. On the other hand, the application of the algorithm described in section 3 enables a considerable reduction of the average grey level variation (0.4833 for the algorithm with gain compensation, and 0.8204 if gain compensation is disabled). As for the pixels' standard deviation (see figure 3 (e)), intervals $[0.5392, 0.7995]$ and $[0.5394, 0.7899]$ are respectively obtained for the algorithm with and without gain compensation. Further results shown in figure 3 are for additive error models computed with $x_0 = 0$. Similar results are also observed for the grey patch image sequence (see figure 4). As expected, for T around $22°C$, all variants of the algorithm perform as Kamberova's method, since in these circumstances the expected noise characteristics are similar. These results suggest that the described method is applicable both (i) to industrial applications of CCD sensors, where usually illumination control and the positioning of the required reference surfaces for gain compensation are feasible, and (ii) to general computer vision tasks, where this conditions are usually not practical or even impossible to implement. In the later case, the gain compensation is not feasible. However, as can be deduced from the shown results, even for cameras with small gain variations, good correction results can be achieved with the proposed strategy without gain compensation. Further, from the above results it can be concluded that BIC_{IC} enables the identification of proper model order to capture the dynamics in offset variation (for this camera an average order model order of 3.48 was obtained), since, when compared to Kamberova's method, (i) all correction results exhibit lower pixel standard deviation and (ii) average intensity variation is drastically reduced (over 90% in the worst case and over 95% in the best case). A typical image after correction is shown in figure 3 (f). As can be observed, this corrected image is smooth. Finally, the use of BIC_{IC} enables the use of a very general imaging model for additive error correction. A sharp imaging model is only required if gain compensation is to be implemented, which in most practical applications is not necessary since usually automatic gain is disabled.

References

[1] Author: To be included. In: To be included. (2001)

[2] Kempen, G., Vliet, L.: The influence of the background estimation on the superresolution properties of non-linear image restoration algorithms. In: Proc. of the Three Dimensional and Multi-Dimensional Mi-

Figure 4. Patch number 19 (white). Correction results for a sequence of 51 images.

croscopy: Image Acquisition and Processing. (1999) 179–189

[3] Willson, R.: Modeling and calibration of automated zoom lenses. Technical Report CMU-RI-TR-94-03, Carnegie Mellon University (1994)

[4] Bubna, K., Stewart, C.: Model selection techniques and merging rules for range data segmentation algorithms. Computer Vision and Image Understanding **80** (2000) 215–245

[5] Schwartz, G.: Estimating the dimension of a model. The Annals of Statistics **6** (1978) 461–464

[6] Craven, P., Wahba, G.: Smoothing noisy data with spline functions. Numer. Math. **31** (1979) 377–403

[7] Neath, A., Cavanaugh, J.: Regression and time series model selection using schwartz information criterion. Communications in Statistics Theory and Methods **26** (1997) 559–580

[8] Chang, Y.C., Reid, J.F.: RGB calibration for color image analysis in machine vision. IEEE Trans. on Image Processing **5** (1996) 1414–1422

[9] Kamberova, G., Bajcsy, R.: Sensor errors and the uncertainties in stereo reconstruction. In: Proc. IEEE Workshop on Empirical Evaluation Techniques in Computer Vision. (1998)

[10] Healey, G.E., Kondepudy, R.: Radiometric CCD camera calibration and noise estimation. IEEE Trans. on Pattern Anal. Machine Intell. **16** (1994) 267–276

[11] Ciarlet, P., Lions, J.: Handbook of Numerical Analysis. Elsevier-North Holland (1990)

[12] Smola, A.: Introduction to Machine Learning. ENGN4520: The Australian National University. (2002)